

Fouling and rejection behavior of ceramic and polymer-modified ceramic membranes for ultrafiltration of oil-in-water emulsions and microemulsions

Ron S. Faibish, Yoram Cohen *

Department of Chemical Engineering, University of California, Los Angeles, CA 90095-1592, USA

Abstract

The effectiveness of poly(vinylpyrrolidone) (PVP)-modification of a zirconia-based ultrafiltration membrane was investigated for the treatment of oil-in-water (o/w) emulsions. Fouling, hydraulic permeability, flux decline, and solute rejection for modified and native membranes were evaluated using a diagnostic o/w emulsion as well as an emulsion prepared using a commercial cutting oil. The native membrane was irreversibly fouled by both the o/w microemulsion and the commercial cutting oil emulsion. In contrast, irreversible fouling was not observed for the PVP-modified membrane. The main fouling agent for the diagnostic o/w microemulsion was identified as the anionic surfactant octanoate, which lead to an irreversible decline of initial membrane hydraulic permeability of up to 20%. Adsorption of surfactant species onto the native membrane surface were attributed to charge screening due to high ionic strength environment and presence of hydroxyl groups on the zirconia surface. Analysis of permeate flux decline and membrane resistance behavior suggests that membrane fouling was mainly due to a solute cake (gel) layer buildup at the membrane surface. However, the possibility of some internal pore plugging, due to deposition of small surfactant molecules, micelles or oil droplets, during the initial few minutes of filtration runs, could not be ruled out. Improved oil rejection (two-fold for the microemulsion and over 20% for the cutting oil emulsion) with the modified membrane compared to the native membrane was attributed to repair (or narrowing) of defects (or ‘pin-holes’) of the native membrane upon polymer grafting. © 2001 Elsevier Science B.V. All rights reserved.

Keywords: Ceramic membranes; Microemulsions; Ultrafiltration

1. Introduction

Fouling of ultrafiltration (UF) and microfiltration (MF) membranes is frequently encountered in

filtration and treatment of colloidal suspensions (e.g., proteins, bacteria, inorganic oxides) and treatment of oil-in-water (o/w) emulsions in environmental applications [1–8]. Membrane fouling results in substantial decline in initial membrane hydraulic permeability, which may be reversible or irreversible (Fig. 1). Reversible permeability decline (i.e., reversible fouling), which is typically attributed to deposited solute or colloidal particles on

* Corresponding author. Tel.: +1-310-8258766; fax: +1-310-2064107.

E-mail address: yoram@ucla.edu (Y. Cohen).

the membrane surface and in the membrane pores, can be readily overcome by mild cleaning [1,2]. On the other hand, irreversible decline of membrane permeability (i.e., irreversible fouling) is often due to strong physisorption and/or chemisorption of particles or solutes onto the membrane surface and in its pores [1,9,10]. Irreversible fouling could become more severe with each additional treatment and cleaning cycle due to further adsorption of foulants onto the membrane surface (Fig. 1). Cleaning of irreversibly fouled membranes requires harsh chemical and/or high temperature thermal treatments; however, often the initial permeability of irreversibly fouled membranes cannot be recovered even with aggressive cleaning methods [1,11,12]. The problem of irreversible membrane fouling is particularly significant in UF of oily waste streams with ceramic membranes, which is the focus of the present study.

Ceramic membranes are particularly suitable for treating often corrosive and high temperature oil- and surfactant-contaminated streams due to the superb mechanical, thermal and chemical stability of such membranes [9,13]. However, irreversible membrane fouling due to adsorption of a wide range of solute species present in oily streams can severely reduce membrane efficiency and lifetime. The problem of fouling in filtration and treatment of oily

aqueous wastes can be particularly severe since such streams contain different amphiphiles (e.g., surfactants and detergents) that can strongly adsorb onto the membrane [12,14,15]. For example, Field et al. [14] showed that reversible and irreversible fouling of ceramic zirconia-coated nickel alloy mesh composite membranes occurred with both anionic (sodium dodecyl sulfate) and nonionic (poly(ethylene glycol) 2025) surfactants, which are often found in oily wastes. In another study, Rajagopalan et al. [15] found that a ceramic membrane was irreversibly fouled by a spent mixture of anionic and ionic surfactants used to clean oily machine parts at a railroad facility; membrane permeability was found to irreversibly decrease by as much as 66%.

Various chemical and physical methods have been proposed to modify membranes in order to reduce membrane fouling and improve solute rejection and permeate flux [10,12,16–25]. However, to date, most membrane modification studies on the minimization of colloidal fouling involved UF and MF polymeric membranes, primarily for the filtration of protein-containing solutions. A limited number of studies have specifically addressed membrane fouling reduction via membrane surface modification for treatment of oil-contaminated waste streams [12,17,26].

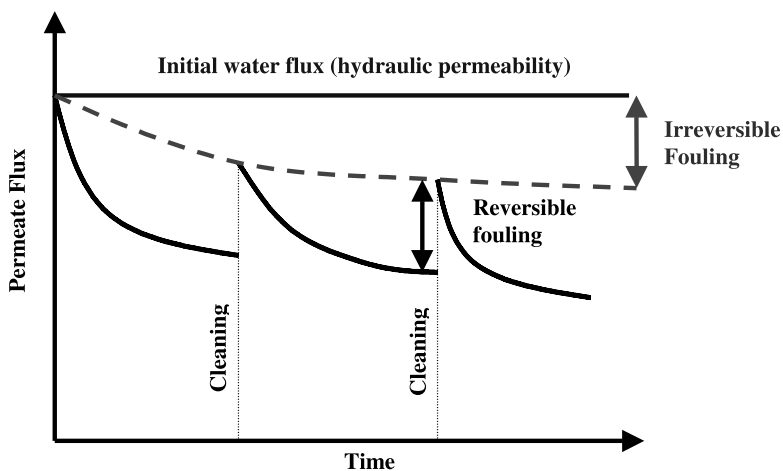


Fig. 1. Illustration of reversible and irreversible permeate flux decline in membrane UF.

For example, Anderson and Saw [17] have shown that membrane preconditioning by physical adsorption of nonionic surfactants onto the surfaces of hydrophilic polymeric UF membranes significantly increased oil rejection when treating a cotton seed o/w emulsion. However, the adsorbed surfactant layer was partially removed during long-term operation and even washed-out completely upon membrane cleaning. Covalent bonding of hydrophilic polymer chains onto the surface of ceramic membranes was also shown to be effective for reducing fouling in the filtration of o/w emulsions while improving oil rejection [12,27]. The performance (i.e., rejection and permeate flux behavior) of the above ceramic-supported polymer membranes was maintained even after numerous filtration and cleaning cycles, thereby demonstrating the stability of the chemically-bonded polymer modifying layer. The above studies, however, did not identify the specific species responsible for fouling of the native (i.e., unmodified) membrane. Clearly, a successful development and optimization of fouling-resistant membranes for o/w filtration, via surface modification, must follow a systematic approach that first identifies the species responsible for fouling and targets a membrane surface modification process to minimize and/or eliminate fouling.

In the present study, we extend earlier work and present a systematic approach for membrane fouling evaluation geared towards the development of a fouling resistant ceramic-based membrane. We first demonstrate, using a well-characterized diagnostic o/w emulsion [12], the extent of expected fouling with the native membrane. Then, we proceed to identify the components responsible for fouling from the combination of equilibrium adsorption experiments and membrane permeability experiments using various components of the emulsion mixture as well as the emulsion itself. An investigation of the performance of a membrane, modified specifically to eliminate performance degradation by the identified foulant, was then carried out and compared to the native membrane, using both diagnostic and commercial o/w emulsions. The ultimate goal of the presented approach is to elucidate the cause of fouling, and thereby allow one to optimize the

specific surface modification approach for reducing fouling and improving membrane rejection and flux performance.

2. Experimental

2.1. Materials

Ultrapure de-ionized (DI) water was obtained by filtering distilled water through a Milli-Q Water System (Millipore Corp., San Jose, CA). NaOH solutions (1 and 0.1 N) and HCl solutions (concentrated, 1 and 0.1 N), *n*-decane (certified), isobutanol (certified, ACS), 30% hydrogen peroxide (certified, ACS), concentrated H₂SO₄, and methylene chloride (GC Resolv.) were purchased from Fisher Scientific (Pittsburgh, PA). Sodium octanoate, octanoic acid and zirconia particles (< 5 μm in size) were obtained from Aldrich Chemicals (Milwaukee, WI). Commercial water-soluble cutting oil, Castrol 329, was obtained from Castrol Industrial Inc. (Los Angeles, CA).

Tubular porous membrane supports consisting of a carbon-supported zirconia membrane (Carbosep membrane), with a manufacturer reported MW cutoff of 15 kDa (average pore size of ≈ 4 nm) and an overall thickness of 0.247 cm, were obtained from Rhodia Orelis (Miribel, France). The average thickness of the active zirconia layer was measured as 2.75 μm [12]. The membrane with inner and outer diameters of 3.00 and 5.29 mm, respectively, was rated by the manufacturer for use over a pH range of 0–14, temperatures exceeding 100 °C, and a maximum operating pressure of 10 bars (1.01 MPa). The specific hydraulic water permeability of the membranes ranged from 1.71×10^{-7} to 3.78×10^{-7} ms⁻¹ Pa⁻¹ at 20 °C.

2.2. Membrane modification

The zirconia membranes were modified via an established two-step reaction with intermediate treatments [12,28–30]. In the first step (i.e., surface activation), vinyltrimethoxysilane (VTMS) was covalently bonded to hydroxyl groups on the zirconia surface. The resulting surface-bound vi-

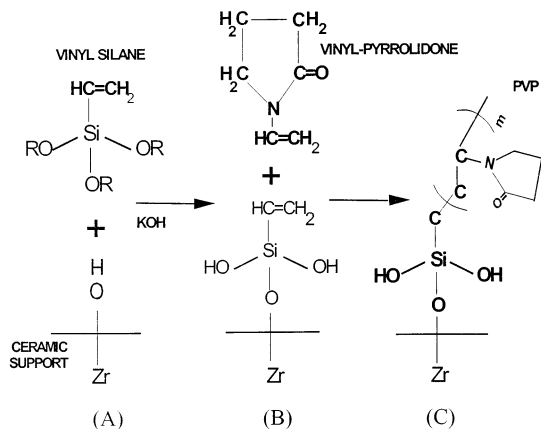


Fig. 2. Steps in VP free-radical graft polymerization onto zirconia or silica surfaces: (A) surface silylation followed by basic hydrolysis of methoxy groups; (B) VP surface grafting; (C) covalently-anchored PVP surface chains.

nyl groups served as the anchoring sites for polymer chains, which were grafted to the surface by free-radical graft polymerization (Fig. 2). Silylation of the wafers or particles with VTMS was carried out for a period of 5 h in a VTMS solution in xylene maintained at just below the boiling point of xylene (~ 134 °C). At the end of the reaction, the membranes were thoroughly rinsed with xylene and oven-dried overnight under vacuum at a temperature of 140 °C. Prior to graft polymerization the membranes were hydrolyzed using a KOH solution (pH 12) to convert unreacted surface methoxy groups to silanols.

Details of the subsequent experimental method for vinylpyrrolidone (VP) graft polymerization can be found elsewhere [12,28,29]. Briefly, graft

polymerization with VP was carried out in an aqueous medium using hydrogen peroxide as initiator. The graft polymerization reaction was carried out for a period of 8 h at different reaction conditions (see footnote in Table 1). At the termination of the reaction, the polymer-modified membranes were thoroughly washed with DI-water to remove adsorbed or entangled PVP chains. The resulting polymer-modified surfaces consisted of poly(vinylpyrrolidone) (PVP) chains, which were terminally anchored to the ceramic substrate (Fig. 2).

2.3. Oil-in-water microemulsions and cutting oil emulsion

O/w microemulsions were prepared by mixing decane (the dispersed phase) and ultrapure DI water with varying amounts of the emulsifying agents (i.e., main surfactant: sodium octanoate (critical micelle concentration (CMC) = 0.4 M [31]); co-surfactants: isobutanol and octanoic acid) to yield a range of nanodroplet sizes. The resultant microemulsions contained nanodroplets in the size range of 18–66 nm with standard deviation (SD) range of 20–39%, as determined by dynamic light scattering (DLS) measurements (Submicron Particle Sizer, Nicomp Model 370, Santa Barbara, CA) and had an average oil content of 3.4×10^4 mg l⁻¹. The size of the surfactant octanoate micelles in a solution of 0.5 M (> CMC) sodium octanoate, which was used in the experimental study, was also determined, using DLS, to be 3.7 nm (SD of 47%). All microemulsions were Newtonian with viscosity ranging from 5.38 to 12.6 mPa s [12].

Table 1

Hydraulic permeability (k_f) of native and PMC membranes before o/w microemulsion filtration experiment and after o/w microemulsion filtration followed by mild caustic (NaOH solution pH ~ 12) cleaning. $T = 20$ °C

Membrane ^a	k_f (10^{-16} m ²) clean membrane	k_f (10^{-16} m ²) after filtration and cleaning	% Reduction
Native	4.70	3.47	26
M10T70	2.89	2.89	0
M30T70	2.67	2.60	<3
M30T80	3.40	3.39	<1

^a The number after M and T in membrane designations refer to initial monomer (VP) concentration and reaction temperature in °C (after Ref. [12]).

Table 2
Composition of Castrol 329 soluble oil

Component	wt.%	CAS number
Distillates (petroleum), hydrotreated heavy naphthenic	5–10	64742-52-5
Alkanes, C12-18, ethoxylated propoxylated	1–5	69227-21-0
Alkanes, chloro	15–20	61788-21-0
Distillates (petroleum), solvent-refined heavy naphthenic	45–50	64741-96-4

Source: product material data safety sheet (MSDS). *Note:* Manufacturer also reported presence of sulfonate surfactants.

A commercial cutting oil emulsion was prepared by mixing 4.5 g Castrol water-soluble cutting oil with 1.5 l (i.e., 3000 mg l⁻¹) ultrapure DI water using a homogenizer (Powergen 700, Fisher Scientific) at a constant speed of 2500 rpm for 2 min. The composition of the cutting oil is given in Table 2. The viscosity of the emulsion at 20 °C, determined using an Ubbelohde viscometer (Cannon Instrument Co., State College, PA), was 1.03 mPa s. The average oil droplet sizes in the feed and permeate solutions were measured by DLS

and found to be in the range of 98–105 nm and 110–120 nm, respectively, with a SD range of 30–60%.

2.4. Adsorption experiments

Native and PVP-grafted zirconia particles (with surface area of 6.1 m² g⁻¹ [12,32]) were used as surrogate substrates to the membrane in order to determine the potential of surfactant or co-surfactants adsorption onto the native or modified surfaces. The particles (0.8 g) were placed in test tubes containing aqueous solutions (8 ml) of the surfactant and co-surfactants with concentrations similar to those in the o/w microemulsion. Control samples contained the above solutions in the absence of particles. The test tubes were continuously agitated for a period of 3 h (the length of a typical filtration experiment). Concentrations of the various species were determined according to the analysis procedures described in Section 2.5. Uptake of species by the particles (i.e., adsorption) was calculated from the difference between the initial and final amounts in solution per unit mass or area of particles.

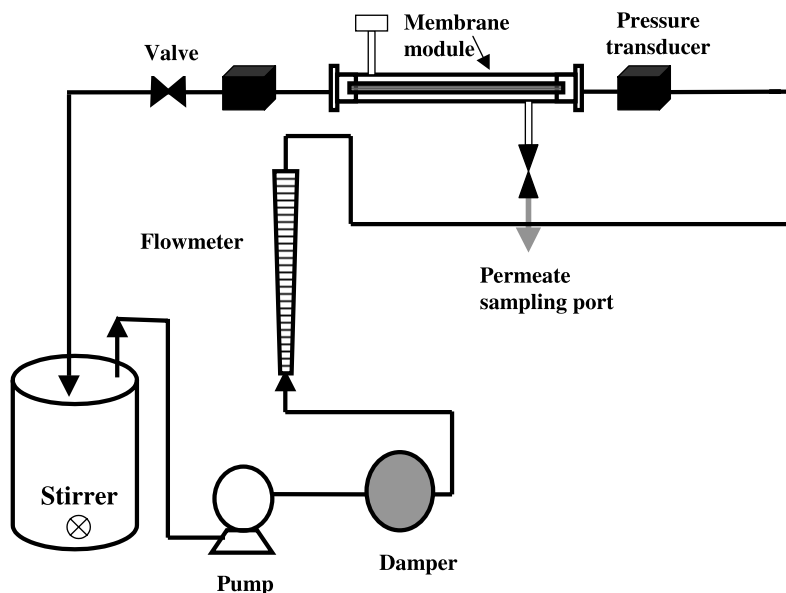


Fig. 3. Membrane filtration system.

2.5. Filtration study

Membrane filtration experiments were conducted to assess the extent of membrane fouling by a number of chemical species. The crossflow filtration system used in the study is shown schematically in Fig. 3. The solution feed flask was immersed in an isothermal water bath and the solution was fed through a flow damper to the inlet port of membrane system using a diaphragm pump (Flojet pump, Cole-Parmer Instrument Co., Vernon Hills, IL). The transmembrane pressure was controlled by a needle valve installed on the outlet side of the membrane module. Transmembrane pressure was monitored by variable reluctance differential pressure transducers (Model DP15-44, Validyne Engineering Corp., Northridge, CA, full-scale error of $\pm 0.5\%$) connected to the outlet and inlet sides of the membrane module. Permeate flux and feed flow rate were measured gravimetrically (AE 200, Mettler Instrument Co., Highstown, NJ) and/or volumetrically by collection of samples over given time periods. Typical filtration experiments using the decane microemulsions, surfactant (0.3 and 0.5 M sodium octanoate) and co-surfactant (2 vol.% isobutanol and 0.002 M octanoic acid) solutions, and Castrol cutting oil emulsion lasted for periods of 60–200, 200–270, and 480–600 min, respectively, until steady-state flux was reached. The concentrations of isobutanol and octanoic acid were below their aqueous solubility limit (about 5 vol.% [33] and 4.7 mM [34] at 25 °C, respectively) to ensure homogeneity of solutions.

Irreversible membrane fouling, with the decane o/w microemulsion, was investigated only for laminar flow conditions (average highest attainable N_{Re} of 570) since operation under turbulent flow conditions was not possible for this high emulsion viscosity with the present filtration system [12]. Correspondingly, fouling experiments with various surfactant and co-surfactants solutions were also conducted under laminar flow conditions ($N_{Re} = 640$). On the other hand, flux decline experiments with the low viscosity (1 mPa s) cutting oil emulsion were conducted for a wide range of N_{Re} (1390–9500) allowable for the current system to cover the full range of potential

practical operating conditions. After each filtration experiment the membrane was cleaned by rinsing it at the maximum allowable flow rate (in a crossflow operation) with DI water and subsequently submerging it in a stirred aqueous solution of NaOH (pH 12) for about 1 h. The membrane was then thoroughly rinsed with DI water. The hydraulic permeability, k_i (m^2), of the membranes was determined by measuring permeate flux as a function of transmembrane pressure and using the following equation [12]:

$$k_i = \frac{J_w \mu_w R_i \ln(R_o/R_i)}{\Delta P_m}, \quad (1)$$

where J_w is the water permeation flux ($m\ s^{-1}$), μ_w is water viscosity (Pa s), R_i and R_o are the inside and outside membrane tube radii (m), respectively, and ΔP_m is the transmembrane pressure (Pa). The hydraulic permeability was calculated for the membranes before and after the filtration experiments and membrane cleaning to assess the impact of irreversible membrane fouling.

Permeate and feed o/w microemulsions samples were analyzed for decane and isobutanol content by extracting 0.5 ml of permeate or feed samples with $3 \times 6\ ml^2$ of methylene chloride [12]. The methylene chloride-rich product solutions were analyzed using a gas chromatograph (HP 5890A GC with a HP 3390 peak integrator, Hewlett-Packard, DE) equipped with a flame ionization detector and a Carbowax 1500 packed column (Supelco, Inc., PA). The samples were analyzed for octanoic acid and sodium octanoate by titrating 0.250 ml samples in 40 ml of methanol to the equivalence point using 0.1 N NaOH and 0.1 N HCl solutions, respectively. Feed and permeate samples of the surfactant and co-surfactant solutions were also analyzed using the above procedures. Concentration of the organic components in the feed and permeate samples of the Castrol 329 emulsions were determined by total organic carbon (TOC) (EPA Method 415.1) and UV absorbance at a wavelength of 262 nm (HP 8452 UV spectrophotometer, Hewlett-Packard, DE) analyses. The above composition analysis enabled the determination of the oil, surfactant, and co-surfactants rejection with an estimated maximum error of $\pm 5\%$.

Table 3
Hydraulic permeability (k_i) of membranes

Component	k_i (10^{-16} m ²) clean membrane	k_i (10^{-16} m ²) after filtration and cleaning	% Reduction
(a)			
4% (by vol.) isobutanol	7.39	7.38	<1
0.002 M octanoic acid	7.39	7.27	2
0.5 M sodium octanoate (>CMC)	7.39	6.12	17
0.3 M sodium octanoate (<CMC)	7.08	5.62	21
Microemulsion	4.40	3.47	26
(b)			
0.5 M sodium octanoate (>CMC)	3.40	3.39	<1
0.3 M sodium octanoate (<CMC)	3.39	3.37	<1
(c)			
Native membrane	7.00	5.80	17
Modified membrane	3.39	3.33	<2

(a) Hydraulic permeability (k_i) of native Carbosep membranes before and after filtration with separate components of the o/w microemulsion itself. (b) Hydraulic permeability (k_i) of modified Carbosep membrane (M30T80) before and after filtration with 0.3 and 0.5 M sodium octanoate solutions. (c) Hydraulic permeability (k_i) of native and modified membrane (M30T80) before and after filtration with the cutting oil emulsion, $T = 20$ °C.

3. Results and discussion

3.1. Microemulsion species responsible for membrane fouling

The first step in the development of a fouling-resistant membrane calls for an initial evaluation of native membrane fouling behavior as previously reported using a well-characterized diagnostic o/w microemulsion [12]. Previous work has shown that after filtration of this decane-based o/w microemulsions, and despite chemical cleaning, the hydraulic permeability of the native membrane was irreversibly reduced by about 26% (Table 1). Irreversible reduction in hydraulic permeability was attributed to irreversible surface adsorption of microemulsion species [12]. Although it was postulated that species with functional groups such as hydroxyls and carboxyls could associate with surface hydroxyls on the zirconia, the specific species were not identified.

In the present study, the first step of identifying potential foulants involved batch adsorption experiments, with solutions of suspected foulants in the o/w microemulsion, for native surrogate zirconia particles. These experiments confirmed significant adsorption of octanoate onto the zirconia

particles (4.0×10^{-4} mol octanoate g⁻¹ particles or 5.8 mg m⁻²). In contrast, no measurable adsorption of octanoic acid or isobutanol onto the native zirconia particles was detected.

Membrane filtration experiments with the various potential foulants confirmed the above findings. An observed irreversible reduction of native membrane hydraulic permeability with sodium octanoate (17–21%, see Table 3a) suggests the adsorption of the anionic octanoate molecules (i.e., the *identified foulant*) onto the zirconia membrane surface and pore walls as a possible reason for the permeability loss (i.e., irreversible membrane fouling). The co-surfactants, isobutanol and octanoic acid, on the other hand, were found not to irreversibly foul the native zirconia membrane. This was confirmed by the insignificant reduction in the clean native zirconia membrane hydraulic permeability (<2%) after filtration experiments with the co-surfactants (Table 3a). The irreversible adsorption of octanoate onto the zirconia surface may be attributed, in part, to association between octanoate and zirconia surface hydroxyl groups, which are known to be present on the zirconia surface at pH levels even higher than the isoelectric point of zirconia (i.e., pH > pI ~ 5.8, when both the zirconia surface and surfactant

molecules are negatively charged) [12,32,35]. Previous studies have also shown that anionic species (e.g., sodium dodecyl sulfate) can adsorb onto negatively charged inorganic oxide surfaces [35,36]. Adsorption was significant when the ionic strength of the solution was high (~ 0.03 M), thereby effectively reduce double layer repulsive forces between the similarly charged surface and surfactant molecules [36]. The ionic strength of the surfactant solutions used in the present study was even higher (0.3–0.5 M), thus, adsorption enhancement due to charge screening is expected, as seen in previous studies [37,38].

Given the above evaluation, it was concluded that, with effective screening of surface hydroxyls it would be possible to create a fouling-resistant membrane. This task was accomplished by modifying the zirconia surface by graft polymerization of VP creating a dense surface of PVP chains [29,32]. Evaluation of the effectiveness of the grafted PVP surface phase was first carried out by batch adsorption experiments with surrogate zirconia particles as described previously (Section 2.4). As expected, the zirconia particles did not reveal any detectable adsorption of isobutanol, octanoic acid or sodium octanoate. A detailed analysis and comparison of the performance of a PVP-modified relative to a native zirconia membrane, are provided in the following sections.

3.2. Fouling mechanism: membrane resistance and flux decline

Insight into the possible fouling mechanisms, and thus effectiveness of the grafted polymer layer, can be obtained by evaluating transient flux decline and membrane resistance during filtration of solutions of the individual foulant species. First, we note, as indicated in Fig. 4, that immediate fouling of the native zirconia membrane is manifested by a rapid initial permeate flux decline for both the 0.3 and the 0.5 M solutions. Flux decline was also observed for the octanoic acid solution; however, the membrane hydraulic permeability was retrieved to about 98% of the initial value. Flux decline due to fouling by the foulant octanoate was less severe with the modified membrane relative to the native membrane (Fig. 5).

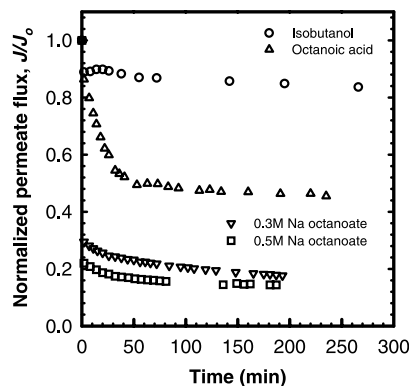


Fig. 4. Transient permeate flux behavior of microemulsion species using the native Carbosep membrane. Experimental conditions: $\Delta P = 68.9$ kPa; $T = 20$ °C; $N_{Re} = 640$.

The fast initial decline is likely to be associated with rapid pore plugging of the membranes, as discussed below.

The mechanism of permeate flux decline for the irreversible fouling due to octanoate can be further analyzed by examining transient variations in total membrane resistance, R_T (m^{-1}), for the native and modified membranes using Darcy's law:

$$J = \frac{\Delta P_m}{\mu(R_T)} = \frac{\Delta P_m}{\mu(R_m + R_i + R_c)}, \quad (2)$$

where J is the permeate flux ($m s^{-1}$), ΔP_m is the transmembrane pressure (Pa), R_m is the intrinsic

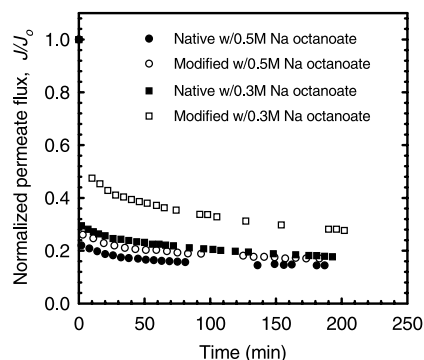


Fig. 5. Transient permeate flux behavior of the main foulant (sodium octanoate) using the native and modified Carbosep membranes above and below the CMC of sodium octanoate. Experimental conditions: $\Delta P = 68.9$ kPa; $T = 20$ °C; $N_{Re} = 640$.

(clean) membrane resistance (m^{-1}) for water flow, R_i is the resistance due to membrane internal fouling (i.e., pore plugging and adsorption) (m^{-1}) determined from $R_i = R_m^f - R_m$ with R_m^f being the membrane resistance after the oil filtration experiment followed by mild cleaning. Finally, R_c is the resistance due to the accumulation of solute near the membrane surface (i.e., solute cake layer) (m^{-1}) calculated from $R_c = R_T - R_m - R_i$. Three main mechanisms for flux decline can be identified for UF of colloidal species as: standard pore blocking, pore blocking and cake buildup [39,40], and these can be, respectively, described by the following resistance models [39]:

$$R_m + R_i = R_m(1 + K_{SPB}Q_o t)^2, \quad (3)$$

$$R_m + R_i = R_m \exp(K_{PB}t), \quad (4)$$

$$R_T = R_m(1 + 4K_{CB}Q_o^2 t)^{1/2} \quad (5)$$

where K_{SPB} , K_{PB} and K_{CB} are constants, t is time, and Q_o is the permeate initial volumetric flow rate. In standard pore blocking, flux decline is due to gradual constriction of pores while the number of available pores remains constant. The pore-blocking model assumes that the pore size remains constant; however, the number of pores decreases with time due to pore plugging. In the cake buildup (or cake filtration) model, internal membrane fouling due to pore plugging does not occur and only R_c increases with time. The total resistance–time curve is concave-up according to Eqs. (3) and (4), while Eq. (5) produces a concave-down curve. In the present study, plots of R_T as a function of time for the native and modified membranes (Fig. 6) all yielded concave-down curves, suggesting that external fouling (i.e., via cake buildup) is the main mechanism for fouling. However, internal fouling due to pore plugging at the very early stages of filtration (i.e., within the first minute of rapid flux decline (Fig. 5)) cannot be ruled out given the small size of octanoate micelles at 0.5 M (3.7 nm, Section 2.3) and the octanoate molecule itself at 0.3 M (in the absence of micelles). It is plausible that a point of inflection in the curves, which would indicate initial upward concavity due to pore blockage, was not detected since it was not possible to measure the permeate flux during the first minute of the filtra-

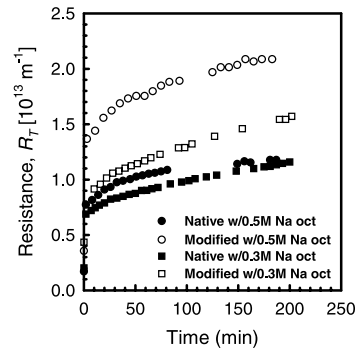


Fig. 6. Transient behavior of total resistance of the native and modified membranes with sodium octanoate solutions above (0.5 M) and below (0.3 M) the CMC of sodium octanoate. Experimental conditions: $\Delta P = 68.9$ kPa; $T = 20$ °C; $N_{Re} = 640$.

tion experiments. It is emphasized, however, that fouling for the modified membrane was completely reversible since membrane initial water flux (or hydraulic permeability) was recovered after mild membrane cleaning (Section 2.5 and Table 3b).

Analysis of the transient total resistance, for the o/w microemulsion system, could not be performed due to extremely low permeate flux for this high viscosity microemulsion. Due to the extremely low flux, flux decline could not be observed for at least the first 30 min of the filtration experiment [12]. Thus, all measurements of permeate flux were essentially at steady state.

3.3. Membrane performance with commercial cutting oil emulsion

In order to demonstrate the more general applicability of the PMC membrane, its performance, relative to the native membrane, was also evaluated with a commercial cutting oil emulsion. The native membrane was irreversibly fouled as indicated by an irreversible hydraulic permeability loss of 17% after filtration with the cutting oil, followed by mild caustic cleaning. In contrast, hydraulic permeability reduction for the modified membrane was low ($< 2\%$, Table 3c) and within the maximum range of experimental error of $\pm 5\%$ (Section 2.4). For both the native and

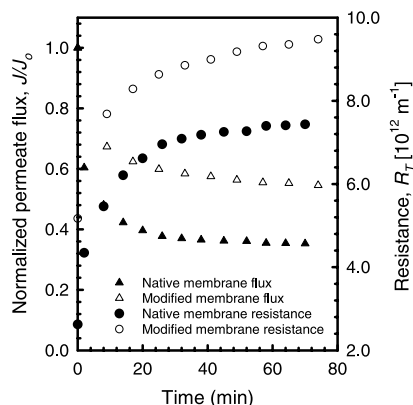


Fig. 7. Transient permeate flux and total resistance for the native and modified membranes with cutting oil emulsion. Experimental conditions: $\Delta P = 68.9$ kPa; $T = 20$ °C; $N_{Re} = 1390$; oil concentration = 3000 mg l^{-1} .

modified membranes, the transient total resistance curve is concave down, suggesting that external membrane fouling by cake layer buildup was the main fouling mechanism (Fig. 7). The oil droplets, for the commercial cutting oil emulsion, were significantly larger than the average membrane pore size (~ 100 vs. ~ 4 nm); therefore, their rejection was high (as high as 98.6%; Table 4) and

as a result their accumulation increased near the membrane surface. If pore blockage did occur, it is not apparent given the lack of an inflection point in the total resistance plots (Section 3.2). Clearly, if pore blockage (or adsorption in the pores of the native membrane) did occur, it should have taken place immediately after the start of the filtration experiment; therefore, the native and modified membrane R_c values reported in Table 5 could possibly include reversible pore blockage effects. It is emphasized, however, that the hydraulic permeability of the modified membrane remained unaltered after filtration of the cutting oil emulsion, suggesting the absence of irreversible pore blockage effects. The above performance of the modified membrane is especially encouraging given the wide range of potential foulants (e.g., surfactants) present in the oil mixture (Table 2).

It is important to note that oil rejection significantly increased for the modified compared with the native membrane by about 5–20% under laminar flow conditions and by about 4–14% for the turbulent region covered ($2380 \leq N_{Re} \leq 9500$) (Table 4 and Fig. 8). Overall rejection by the native membrane was as low as 74% for oil and

Table 4
Flux and rejection results

N_{Re}	Permeate steady-state flux (10^{-6} m s^{-1})		% TOC rejection ^a		% Oil rejection ^b	
	Native	Modified	Native	Modified	Native	Modified
(A)						
Initial water flux	26.3	13.3	–	–	–	–
1390	9.27	7.27	72	93	74.3	95.5
2380	10.3	8.16	80	92	82.9	96.5
4160	14.4	10.3	88	96	89.4	97.5
5500	19.2	10.7	89	94	91.5	97.7
7420	21.4	11.2	88	95	92.4	97.9
9500	22.6	12.1	90	95	92.4	97.9
(B)						
1390	5.51	3.35	90	95	93.4	98.6
4160	6.70	3.67	93	97	94.8	98.6
6100	7.36	3.91	89	96	94.8	98.2

Flux and rejection results for both native and PVP-modified membranes with cutting oil emulsion for a range of N_{Re} and two transmembrane pressure conditions: (A) 68.9 and (B) 27.6 kPa. Oil concentration = 3000 mg l^{-1} ; $T = 20$ °C.

^a Obtained from TOC analysis (EPA Method 415.1, Section 2.4).

^b Obtained from UV absorbance measurements (Section 2.4).

Table 5

Percent contribution of cake layer resistance (R_c) to total membrane resistance (R_T)

N_{Re}	R_T (10^{12} m^{-1})		R_c (10^{12} m^{-1})		$(R_c/R_T) \times 100$	
	Native	Modified	Native	Modified	Native	Modified
(A)						
1390	7.43	9.48	4.39	4.31	59.1	45.4
2380	6.68	8.44	3.64	3.27	54.5	38.8
4160	4.79	6.69	1.75	1.52	36.5	22.7
5500	3.59	6.43	0.554	1.26	15.4	19.5
7420	3.22	6.15	0.182	0.978	5.6	15.9
9500	3.04	5.71	0.005	0.540	0.2	9.5
(B)						
1390	5.04	8.34	2.00	3.17	39.7	38.0
4160	4.17	7.63	1.13	2.46	27.1	32.2
6100	3.79	7.00	0.755	1.83	19.9	26.1

Calculated from the resistance in series model (Eq. (2) Section 3.2) with $R_{m,native} = 2.61 \times 10^{12} \text{ m}^{-1}$; $R_{m,mod} = 5.30 \times 10^{12} \text{ m}^{-1}$; $R_{i,native} = 4.15 \times 10^{11} \text{ m}^{-1}$. Percent contribution of R_c to R_T for both native and PVP-modified membranes with cutting oil emulsion for a range of N_{Re} and two transmembrane pressure conditions: (A) 68.9 and (B) 27.6 kPa. Oil concentration = 3000 mg l^{-1} ; $T = 20 \text{ }^\circ\text{C}$.

72% based on TOC (Table 4). Given that the average oil droplet size, 110–120 nm, was larger than the average membrane pore size (4 nm), it is plausible that defects (large pores) or ‘pin-holes’ could have been responsible for leakage through the membrane, thus, lowering the overall rejection. Indeed, previously reported SEM images of the inner surface of this membrane [12] revealed uneven coverage of the carbon support by the zirconia layer, suggesting the possible presence of pin-holes. Given the significantly higher rejection of ~ 95 –99% by the modified membrane (Table 4 and Fig. 8), it is believed that any ‘pin-holes’ in the native membrane were likely to have been effectively ‘repaired’ (i.e. narrowed in size) by the grafting of PVP chains onto the membrane pore walls.

Analysis of permeate flux decline, expressed as normalized flux (i.e., the ratio of permeate flux to initial clean membrane water flux), is useful to distinguish between initial intrinsic differences in membrane properties prior to contact with the emulsion solution (e.g., different initial hydraulic permeability of native membranes). Normalized permeate flux decline for the modified membrane, under laminar flow conditions, was less severe (22% higher steady-state normalized flux) than for the native membrane (Fig. 9). This was despite the

higher overall membrane resistance of the modified membrane resulting from narrowing of membrane pores upon polymer grafting. Therefore, it is suggested that the higher normalized flux, for the modified membrane, was due to reduction in pore blockage by penetration of oil droplets, since the polymer grafting procedure was most likely effective in ‘repairing’ pore defects.

The difference in normalized flux for the two membranes (native and modified) diminished with increasing tube-side N_{Re} (Fig. 9). Although for the

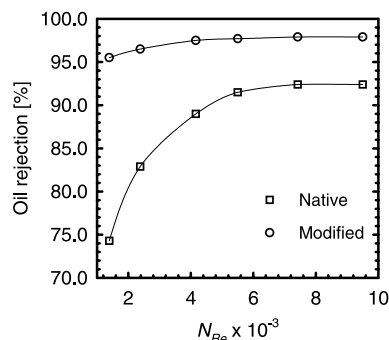


Fig. 8. Effect of Reynolds number on rejection of cutting oil emulsion droplets. Experimental conditions: $T = 20 \text{ }^\circ\text{C}$; $\Delta P = 68.9 \text{ kPa}$; oil concentration = 3000 mg l^{-1} .

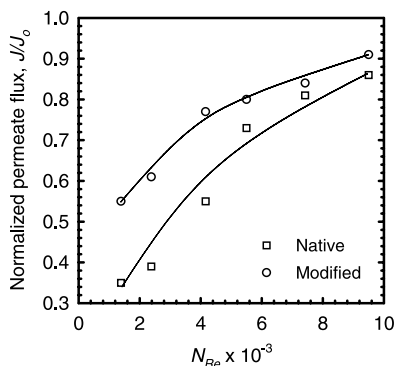


Fig. 9. Dependence of normalized permeate flux on Reynolds number for the cutting oil emulsion for a range of N_{Re} . Experimental conditions: $T = 20$ °C; $\Delta P = 68.9$ kPa.

modified membrane there was a measurable flux decline (upto $\sim 45\%$) in the low N_{Re} region ($N_{Re} < 7420$), over 91% of the flux was recovered. For the native membrane, only 85% of the flux was recovered as the highest N_{Re} of 9500 was approached (Fig. 9). We note that with increasing N_{Re} (i.e., crossflow velocity, V) for both membranes (Table 4; Fig. 9) in the laminar flow regime, the fluid shear stress, $\tau_w = \mu(8V/D)$, exerted at the membrane surface increases, thereby leading to a thinning (thickness decrease) of the oil droplets cake (or gel) layer. The above was manifested by an overall decrease in R_c (Eq. (3)) with increasing N_{Re} , which resulted in an increase in permeate flux (Table 4 Figs. 8 and 9). Blockage of large pores (and possible pin-holes in the native membrane) by surface-deposited oil droplets could explain the higher R_c/R_T ratio for the native membrane (by about 14–16%) at lower N_{Re} (< 5500) (Table 5). The repair (or plugging) of large pores (and/or ‘pin-holes’) by the grafted PVP is also suggestive from the high oil rejection by the modified membrane for the current N_{Re} range (Fig. 8). Higher oil rejection for the modified membrane, for which greater accumulation of oil droplets in the cake layer is expected, may also be the reason for the higher percent contribution of cake resistance to overall resistance at $N_{Re} > 5500$ relative to the native membrane (Table 5).

It is especially encouraging that the present polymer-modified ceramic membrane yielded a

higher permeate flux, relative to the initial water flux (i.e., higher normalized flux), and higher oil rejection compared to the native membrane under both *laminar* and *turbulent* flow conditions (Figs. 8 and 9). The benefit of the above is that operation of the modified membrane, under laminar or low N_{Re} crossflow conditions, would require less pumping power at an equivalent oil rejection, thus, reducing process energy costs. It is important to note, however, that membrane permeability is reduced upon polymer modification. Therefore, in order to optimize the membrane for full-scale applications one would have to select a starting native membrane pore size that upon modification would result in the desired range of membrane permeability and rejection.

4. Conclusions

A systematic investigation of o/w emulsion UF with a zirconia-based membrane revealed that the anionic surfactant was responsible for the majority of the observed fouling. For the specific diagnostic microemulsion used in the present study, adsorption of the anionic surfactant (i.e., octanoate) was linked to possible association of the surfactant’s carboxyl functional group with hydroxyls and negatively-charged surface sites, which were screened by high concentration of counterions (ionic strength range of 0.3–0.5 M). Irreversible fouling by other potential microemulsion foulants (i.e., isobutanol and octanoic acid) was negligible ($< 2\%$). Analysis of flux decline suggests that permeate flux decline due to surfactant adsorption inside the native membrane pores occurred at the very start of the filtration experiment. The native zirconia membrane was also irreversibly fouled (i.e., 17% irreversible decrease in hydraulic permeability) when used to treat an o/w emulsion made of a commercial cutting oil. Irreversible permeability loss did not occur with the PVP-modified membrane for neither the commercial cutting oil emulsion nor the decane-based diagnostic microemulsion. Oil rejection was higher for the polymer-modified membrane (by as much as 22%) than for the native membrane, especially under laminar crossflow conditions. Im-

proved rejection of oil droplets for the modified, relative to the native membrane, suggests that pore defects (i.e., ‘pin-holes’ and other large pores) were ‘repaired’ (or narrowed) by the grafted polymer chains; thus, passage of oil droplets through the modified membrane was reduced. Finally, reversible fouling of the modified membrane was mainly due to external fouling (i.e., cake layer buildup) and any fouling due to pore plugging (if at all) occurred in the first few minutes of filtration. Current work is ongoing to explore the optimization of the PVP-based membrane by investigating the impact of polymer chain size to diameter ratio (for different solvent power conditions) and selection of initial native membrane pore size.

References

- [1] S.S. Kulkarni, E.W. Funk, N.N. Li, Ultrafiltration, in: W.S.W. Ho, K.K. Sirkar (Eds.), *Membrane Handbook*, Van Nostrand Reinhold, New York, NY, 1992.
- [2] L.J. Zeman, A.L. Zydney, *Microfiltration and Ultrafiltration: Principles and Applications*, Marcel Dekker, New York, 1996.
- [3] B. Tansel, J. Regula, R. Shalewitz, Treatment of fuel oil and crude oil contaminated waters by ultrafiltration membranes, *Desalination* 102 (1995) 301.
- [4] A.G. Fane, C.J.D. Fell, A review of fouling and fouling control in ultrafiltration, *Desalination* 62 (1987) 177.
- [5] S. Lee, Y. Aurelle, H. Roques, Concentration polarization, membrane fouling and cleaning in ultrafiltration of soluble oil, *J. Membr. Sci.* 19 (1984) 23.
- [6] P. Lipp, C.H. Lee, A.G. Fane, C.J.D. Fell, A fundamental study of the ultrafiltration of oil-water emulsions, *J. Membr. Sci.* 36 (1988) 161.
- [7] M. Cheryan, N. Rajagopalan, Membrane processing of oily streams: wastewater treatment and waste reduction, *J. Membr. Sci.* 151 (1998) 13.
- [8] G. Belfort, R.H. Davis, A.L. Zydney, The behavior of suspensions and macromolecular solutions in crossflow microfiltration: review, *J. Membr. Sci.* 96 (1994) 1.
- [9] R.R. Bhavé, H.L. Fleming, Removal of oily contaminants in wastewater with microporous alumina membranes, *AIChE Symp. Ser.* 84 (1988) 19.
- [10] H. Ma, C.N. Bowman, R.H. Davis, Membrane fouling reduction by backpulsing and surface modification, *J. Membr. Sci.* 173 (2000) 191.
- [11] E. Matthiasson, B. Sivik, Concentration polarization and fouling, *Desalination* 35 (1980) 59.
- [12] R.S. Faibish, Y. Cohen, Fouling-resistant ceramic-supported polymer membranes for ultrafiltration of oil-in-water microemulsions, *J. Membr. Sci.* 185 (2001) 129.
- [13] W. Doyen, W. Adriansens, B. Molenberghs, R. Leysen, A comparison between polysulfone, zirconia and organo-mineral membranes for use in ultrafiltration, *J. Membr. Sci.* 113 (1996) 247.
- [14] R. Field, S. Hang, T. Arnot, The influence of surfactant on water flux through microfiltration membranes, *J. Membr. Sci.* 86 (1994) 291.
- [15] N. Rajagopalan, R.P. Andes, I.S. Han, J.M. Pickowitz, T.C. Lindsey, W. Wu, C.P.L. Barkan, Evaluation of ultrafiltration for recycling alkaline cleaners at railroad facilities, Report R-904, Association of American Railroads, April 1998.
- [16] R. Schnabel, W. Vulont, High-pressure techniques with porous glass membranes, *Desalination* 24 (1978) 249.
- [17] G.K. Anderson, C.B. Saw, Oil/water separation with surface modified membranes, *Environ. Technol. Lett.* 8 (1987) 121.
- [18] L. Millesime, J. Dulieu, B. Chaufer, Protein retention with modified and unmodified inorganic ultrafiltration membranes: model of ionic strength controlled retention, *J. Membr. Sci.* 108 (1995) 143.
- [19] M. Ulbricht, G. Belfort, Surface modification of ultrafiltration membranes by low temperature plasma II. Graft polymerization onto polyacrylonitrile and polysulfone, *J. Membr. Sci.* 111 (1996) 193.
- [20] D. Lucas, M. Rabiller-Baudry, F. Michel, B. Chaufer, Role of the physico-chemical environment on ultrafiltration of lysozyme with modified inorganic membrane, *Coll. Surf.* 136 (1998) 109.
- [21] P. Aptel, J. Cuny, J. Jozefowicz, G. Morel, J. Neel, Liquid transport through membrane prepared by grafting of polar monomers onto poly(tetrafluoroethylene) films. I. Some fractionations of liquid mixtures by pervaporation, *J. Appl. Polym. Sci.* 16 (1972) 1061.
- [22] P. Aptel, J. Cuny, J. Jozefowicz, G. Morel, J. Neel, Liquid transport through membrane prepared by grafting of polar monomers onto poly(tetrafluoroethylene) films. II. Some factors determining pervaporation rate and selectivity, *J. Appl. Polym. Sci.* 18 (1974) 351.
- [23] H. Iwata, T. Matsuda, Preparation and properties of novel environment-sensitive membranes prepared by graft polymerization onto a porous membrane, *J. Membr. Sci.* 38 (1988) 185.
- [24] J. Randon, P. Blanc, R. Paterson, Modification of ceramic membrane surfaces using phosphoric acid and alkyl phosphoric acids and its effects on ultrafiltration of BSA protein, *J. Membr. Sci.* 98 (1995) 119.
- [25] V. Chen, A.G. Fane, C.J.D. Fell, The use of anionic surfactants for reducing fouling of ultrafiltration membranes: their effects and optimization, *J. Membr. Sci.* 67 (1992) 249.
- [26] A. Hamza, V.A. Pham, T. Matsuura, J.P. Santerre, Development of membranes with low surface energy to reduce fouling in ultrafiltration applications, *J. Membr. Sci.* 131 (1997) 217.
- [27] R.P. Castro, Y. Cohen, H.G. Monbouquette, Silica-supported polyvinylpyrrolidone filtration membranes, *J. Membr. Sci.* 115 (1996) 179.

- [28] M. Chaimberg, Y. Cohen, Free radical graft polymerization of vinylpyrrolidone onto silica, *Ind. Eng. Chem. Res.* 30 (1994) 2534.
- [29] Y. Cohen, R.S. Faibish, M. Rovira, Polymer-modified silica resins for aqueous size exclusion chromatography, in: E. Pefferkorn (Ed.), *Interfacial Phenomena in Chromatography*, Marcel Dekker, New York, 1999.
- [30] Y. Cohen, W. Yoshida, V. Nguyen, J.-D. Jou, N. Bei, Surface modification of oxide surfaces by graft polymerization, in: J. Wingrave (Ed.), *Oxide Surfaces*, Marcel Dekker, New York, in press.
- [31] B. Lindman, G. Lindblom, H. Wennerstrom, H. Gustavsson, Ionic interactions in amphiphilic systems studied by NMR, in: K.L. Mittal (Ed.), *Micellization, Solubilization, and Microemulsions*, vol. 1, Plenum, New York, 1977.
- [32] M. Rovira-Bru, F. Giralt, Y. Cohen, Protein adsorption onto zirconia modified with terminally grafted polyvinylpyrrolidone, *J. Coll. Interface Sci.*, 235 (2001) 70.
- [33] S. Budavari (Ed.), *The Merck Index*, 11th ed., Merck and Co, NJ, 1989.
- [34] C. Jonsson, A.-S. Jonsson, Influence of the membrane material on adsorptive fouling of ultrafiltration membranes, *J. Membr. Sci.* 108 (1995) 79.
- [35] S. Dumon, H. Barnier, Ultrafiltration of protein solutions on ZrO_2 membranes. The influence of surface chemistry and solution chemistry on adsorption, *J. Membr. Sci.* 74 (1992) 289.
- [36] P. Mukerjee, A. Anavil, Adsorption of ionic surfactants to porous glass: the exclusion of micelles and other solutes from adsorbed layers and the problem of adsorption maxima, in: K.L. Mittal (Ed.), *Adsorption at Interfaces*, ACS Symposium Series 8, ACS, Washington, DC, 1975.
- [37] P. Bacchin, P. Aimar, V. Sanchez, Model for colloidal fouling of membranes, *AIChE J.* 41 (1995) 368.
- [38] P. Bacchin, P. Aimar, V. Sanchez, Influence of surface interaction on transfer during colloid ultrafiltration, *J. Membr. Sci.* 115 (1996) 49.
- [39] E.M. Tracey, R.H. Davis, Protein adsorption of track-etched polycarbonate microfiltration membranes, *J. Coll. Interface Sci.* 167 (1994) 104.
- [40] J. Mueller, Y. Cen, R.H. Davis, Crossflow microfiltration of oily water, *J. Membr. Sci.* 129 (1997) 221.